IJMF 869
4 December 2002 Disk used
ARTICLE IN PRESS
No. of Pages 22, DTD = 4.3.1
SPS, Chennai

PERGAMON
International Journal of Multiphase Flow xxx (2002) xxx–xxx
International Journal of Multiphase Flow
www.elsevier.com/locate/ijmulflow

Buoyancy-driven instability of bubbly layers: analogy with thermal convection

M.C. Ruzicka [a,*], N.H. Thomas [b]

[a] Institute of Chemical Process Fundamentals, Czech Academy of Sciences, Rozvojova 135, 16502 Prague, Czech Republic
[b] FRED Ltd., Aston Science Park, Birmingham B7 4BJ, UK

Received 29 January 2001

Abstract

An analogy has been established between the buoyancy-driven instability of thermal layers (Rayleigh–Benard instability) and bubbly layers (homogeneous–heterogeneous regime transition). On the physical level, the analogy is a simple scaling theory based on a suitable definition of the Rayleigh, Prandtl, and Nusselt numbers for bubbly layers. The analogy yields a stability criterion in terms of the critical voidage. The criterion predicts the destabilizing effect of layer dimensions, both the height and width, and the stabilizing effect of the liquid viscosity and hydrodynamic bubble diffusivity. The predictions are in agreement with available experimental data from water–air bubbly layers. On the formal level, the analogy is based on similarities between the governing equations of thermal and bubbly layers. It is shown, how the equations of bubbly layers can be converted into those of thermal layers, provided that the bubble inertia and slip speed are negligible. The suggested analogy applies generally to dispersed two-phase systems controlled by buoyancy, viscosity, and hydrodynamic diffusion (e.g. sedimentation and fluidization).
© 2002 Published by Elsevier Science Ltd.

1. Introduction

The breakdown of buoyant fluid layers by the buoyancy-driven (or: overturning, convective) instability is a classical problem of fluid mechanics (e.g. Chandrasekhar, 1961; Turner, 1979). The basic state is overturned when the buoyancy forces overcome the stabilising effect of viscosity and diffusion. It happens at a critical value of the Rayleigh number, which is the key control parameter

* Corresponding author: Tel.: +420-2-20390299; fax: +420-2-20920661.
E-mail addresses: ruzicka@icpf.cas.cz (M.C. Ruzicka), neale@thomas.net (N.H. Thomas).

0301-9322/02/$ - see front matter © 2002 Published by Elsevier Science Ltd.
PII: S0301-9322(02)00150-7

UNCORRECTED PROOF

of the system. The convective instability is typical for thermal layers, where it has been studied for a long time and the research area is well established. The purpose of this paper is to show that the same phenomenon exists also in dispersed two-phase layers. Large-scale circulatory motions set in these layers at a critical buoyancy input and the corresponding flow regime transition can be treated by the formalism developed for thermal layers. One-phase and two-phase convective systems are briefly reviewed in this section. Attention is paid to the confining lateral walls, whose effect on the instability is substantial.

The typical representative of one-phase systems is the Rayleigh–Benard convection, where a fluid layer enclosed between two horizontal plates is heated from below (e.g. Koschmieder, 1993). The question is when the basic state of rest with a linear temperature (density) profile becomes unstable with respect to buoyant disturbances and the convective circulations set in. The onset occurs at a critical value of the Rayleigh number, Ra_c The governing equations of the thermal system are well-known and the value of Ra_c as well as the character of the circulations depend on the properties of the boundaries. The linear stability analysis of the horizontally infinite thermal layer with free–free (slip) horizontal boundaries was performed by Rayleigh (1916) and with rigid–rigid (no-slip) boundaries later by Jeffreys (1928). The results are extensively discussed by Chandrasekhar (1961) and Drazin and Reid (1981). At Ra_c the layer becomes unstable via the symmetry-breaking supercritical bifurcation, when the overturning buoyancy forces on the disturbance overcome the stabilizing viscous forces. The critical wavenumber can be realized by many steady convective patterns (rolls, cells, rings). For a supercritical $Ra > Ra_c$, a whole continuum of wavenumbers emerges. Further development of the flow with increasing energy input proceeds via a sequence of bifurcations, from steady, through time-dependent oscillatory, to complex and irregular motion (Busse, 1985). An important energy balance theorem relates to the onset (Chandrasekhar, 1961): the convection starts at the lowest temperature gradient across the layer that provides enough buoyant energy to keep the dissipative motion going. Therefore, layers with more friction withstand larger temperature gradients and thus are more stable.

Lateral walls stabilize the thermal layers by limiting the mode spectrum remarkably and by bringing additional viscous friction. Horizontally finite layers confined in enclosures present a difficult mathematical problem. Pellew and Southwell (1940) performed the stability analysis for a rectangular box with slip walls. Davis (1967) considered a more realistic case of a box with rigid walls. Charlson and Sani (1970) studied convection confined in a rigid cylinder. In all these cases, a substantial increase of Ra_c with the layer aspect ratio $A = H/D$ (height H, width D) was predicted theoretically. The increase was observed in numerous experiments with both rectangular and circular enclosures (e.g. Catton and Edwards, 1967; Stork and Muller, 1972, 1975).

Besides confined layers heated from bellow, other situations have been studied too, for instance, unbounded layers, layers of infinite vertical extent, layers heated from a side. Also, a variety of density profiles have been considered. These situations, however, do not relate directly to our subject, a bounded uniform bubbly layer sparged from below.

The passage from one-phase to two-phase systems consists in realizing that the thermal layer is only a special case of buoyant layers. Besides heat, the buoyant effects can be produced by nonuniformities in spatial distribution of other agents present in the fluid, e.g. solute, bubbles, drops, and solids. Batchelor and Nitsche (1991) pointed out that in the case of a solute and very fine dispersed particles, the relative motion between the buoyant agent and the fluid is negligible and the (convection–diffusion) equation of heat may be replaced by formally the same equation of

the dispersed phase concentration. Then, the governing equations of thermal and dispersed layers are equivalent and the Rayleigh number naturally results from the scaling (Batchelor and Nitsche, 1991, 1993; Tong and Ackerson, 1998). Batchelor and Nitsche (1993) found the stabilizing effect of lateral walls on stratified layers with dispersed fine particles. The open question is how well the assumption of zero relative motion applies to real dispersed layers with nonzero particle slip speed and inertia effects in both phases.

There are many studies on the stability of the uniform basic state of a dispersion in 1D arrangement (cross-section average assumed). Much effort has been spent on formulating and analysing the governing equations for 1D two-phase flows, e.g. sedimentation, fluidization, and bubbly flows. The first instability mode usually takes a form of planar concentration waves of various kinds, both kinematic and dynamic in nature (e.g. Kynch, 1952; Wijngaarden and Kapteyn, 1990). Further, 2D and 3D patterns start to appear in originally 1D flow.

There are only few studies on the convective instability of dispersed layers, which essentially is a 2D phenomenon. Jackson and co-workers investigated the convective character of the instability that breaks a uniform fluidized bed (Medlin et al., 1974). They applied the procedure used for the Rayleigh–Benard problem to the fluidized bed equations, with the Froude number as the dimensionless parameter. They found a strong stabilizing effect of vertical walls, which is typical for thermal layers. This effect was later confirmed by experiments (Agarwal et al., 1980). Further, they found that the pressure drop across the bed support increased the bed stability. Also, the liquid-fluidized bed was more stable than the gas-fluidized bed—this does not have a direct analogue in thermal systems and clearly indicates a destabilizing effect of the particle inertia. Shnip et al. (1992) (see also Joshi et al., 2001) performed the linear stability analysis of the 2D uniform bubbly layer and found a criterion for the onset of the circulatory regime. Despite the very simplistic governing equations, with the Reynolds and Froude numbers, they also found the stabilizing effect of vertical walls and pressure drop across the gas distributor. They expected their results to be valid also for fluidized beds.

Besides the above mentioned stability analysis, there are several other attempts at making a link between thermal and dispersed layers. Rothman and Kadanoff (1994) studied behaviour of bubbly layers numerically, with 2D gas-lattice cellular automata, from the point of view of nonequilibrium patterns formation. Depending on the values of the Peclet number and voidage, they observed two kinds of instability of a quasi-equilibrium bubbly mixture, the coarsening instability known from sedimentation and the convective instability leading to large-scale circulations similar to thermal convection cells. Kimura and Iga (1995) explored convection in thin liquid layers sparged with gas both experimentally and numerically. They performed experiments with electrochemically generated microbubbles. With increasing the gas production rate, the following typical behaviour was observed in 2D configuration: isolated bubble chains, mushroom-like plumes form chains mergers, convective cells produced by plumes, no ordered motions. In 3D experiments, unsteady irregular patterns typically occurred. In 2D simulations, two-fluid governing equations were used. They were similar to the thermal equations, but the bubble diffusion was replaced with the bubble advection. The Rayleigh and Prandtl numbers resulted from the scaling. The calculations revealed that the mushroom-like plumes were created by the Rayleigh–Taylor instability of the interphase between the bubbly mixture (light phase) rising below the pure liquid (heavy phase) at the initial stage of sparging. When these plumes reached the surface, steady convective cells were established with various aspect ratio, depending on values of Ra and Pr.

UNCORRECTED PROOF

Climent and Magnaudet (1999) addressed a similar problem like Kimura and Iga (1995). The origin of large-scale motions in developing bubbly layers in a 2D box was investigated numerically by large-scale simulations. Meso-scale filtered Navier–Stokes equations were used for the liquid and the Lagrangian approach for individual bubbles. They observed two different flow regimes, without and with large-scale motions, depending on the voidage and the bubble residence time. In the former regime, the rising interphase between the bubbly mixture and the pure liquid remained flat. In the latter regime, the interphase became unstable and developed into mushroom-shape fingers of large bubble concentration, resulting in intense upwelling motions—the Rayleigh–Taylor instability. A long-term picture of already developed layers displayed circulatory cells, similar to those in thermal convection. To characterize the two flow regimes, the Rayleigh and Prandtl numbers were defined similarly like in Kimura and Iga (1995). *Pr* was set constant. *Ra* varied and its critical value was determined. Tong and Ackerson (1998) investigated a possible analogy between fluctuations in colloidal sedimentation and turbulent thermal convection theoretically. Coarse-grained creeping-flow equation was used for the fluid and the diffusion equation for the particle concentration, with Prandtl and Rayleigh numbers as the control parameters. Their sedimentation equations were equivalent to the thermal equations and they thus expected the same structure of the fluctuations at high *Pr* and *Ra*. They also realized that, unlike the thermal layers, no large-scale density gradient responsible for unstable stratification exists in the sedimenting layers. Instead, the flux of the dispersed particles through the layer is kept constant and the nonuniformities, which trigger the onset of convection, result from hydrodynamic interactions among the particles and between the particles and the induced flow. All these studies are valuable and highly inspiring, highlighting certain aspects of the analogy. On the other hand, other important aspects are not taken into account. For instance, the hydrodynamic bubble diffusion is not considered and the layers are not homogeneous (early stages of sparging). Further, the numerical simulations bear a fingerprint of the particular governing equations used and are usually limited to 2D cases. Finally, a direct quantitative support by experiments is lacking.

Our main goal is to establish the bubbly-thermal analogy on the basis of generic physical similarities. This approach avoids the necessity of knowing the governing equations and the result is directly testable by real 3D experiments. Therefore, some basic facts about bubbly layers are presented here.

Bubbly layers confined in containers, i.e. bubble columns with zero net liquid flux, have been studied by chemical engineers for a long time (Deckwer, 1992; Kastanek et al., 1993). It is the well-established fact, that there are two basic flow regimes, homogeneous and heterogeneous (or: uniform and circulatory) (Zahradnik et al., 1997; Joshi et al., 1998). The *homogeneous regime* is characterized by the absence of large-scale motions, the circulations. The homogeneous bubble bed is composed of roughly monodisperse bubbles rising almost vertically with small fluctuations in positions and velocities. The voidage distribution is statistically uniform in space and time. The collectively rising bubbles generate a small-scale randomly fluctuating liquid velocity field with near zero long-term average. Thus, the homogeneous regime presents a uniform basic state of the long-term rest (conductive regime).

On the other hand, the *heterogeneous regime* displays intense large-scale motions. The heterogeneous bubble bed contains pronounced nonuniformities in the voidage and velocity distributions due to the strong coupling between the gas and liquid phases. Voidage disturbances resulting from hydrodynamic bubble–bubble interactions trigger and drive vigorous convective

motions of the liquid on scales comparable with the column size, where highly buoyant regions are accelerated and advected to the top. As a feedback, these liquid motions cause the heterogeneity of the primary voidage distribution at the sparger. Both the voidage and velocity fields are highly unsteady (Chen et al., 1994). After taking the long-term average, these fields show steady, roughly parabolic profiles with maxima in the central part of the column (Hills, 1974; Franz et al., 1984). The time averaged liquid flow field displays smooth circulation loops (Lapin and Lubbert, 1994) similar to those in thermal convection. These loops are the result of the averaging process and, therefore, are not generally visible by naked eyes in real columns. However, they can be observed directly, for instance, in flat quasi-2D columns, where the occurrence of counter-rotating circulation cells were reported (Chen et al., 1989). The steady loop structure of the flow is frequently assumed in models of bubble columns (Joshi and Sharma, 1979). The heterogeneous bubble bed can contain polydisperse bubbles due to the coalescence and breakup (Prince and Blanche, 1990). Thus, the heterogeneous regime presents a nonuniform state with long-term circulations (convective regime).

Under certain conditions (suitable gas distributor, column dimensions, physico-chemical properties of the phases) both regimes can be obtained in the same equipment (Zahradnik et al., 1997). The homogeneous regime exists at low gas inputs (up to 5 cm/s of the superficial gas velocity, say) and is stable with respect to small disturbances of the voidage and velocities The uniformity is recovered by hydrodynamic bubble–bubble interactions, namely by the process of the hydrodynamic bubble diffusion, which prevents the bubbles from forming highly buoyant clusters. When increasing the buoyant energy input, a gradual transition to the heterogeneous regime occurs (Mudde and Akker, 1999). The large-scale motions occupy still larger and larger portion of the column, till they fill the column completely. The critical point where the homogeneous regime loses its stability and the transition begins (the circulations start to appear first) can be determined from experimental voidage-gas flow rate data in several ways (Ruzicka et al., 2001a). For instance, the classical drift-flux plot method by Wallis (1969) is reliable and accurate. Thus, the homogeneous–heterogeneous regime transition is the transition from the absence to the presence of the large-scale motions in a uniform bubbly layer (onset of convection).

Consequently, the bubbly-thermal analogy can be based on the following generic similarities:

- large-scale motions are absent in the conductive regime;
- large-scale motions are present in the convective regime;
- the onset is triggered by a density disturbance;
- the critical point is obtainable from experimental data.

The paper is organized as follows. In Section 2.1, the bubbly-thermal analogy is established on the physical basis. The thermal formalism is presented and the Rayleigh number is defined in terms of forces. On this grounds, this key number is newly introduced for bubbly layers and a stability criterion is obtained. In Section 2.2, the bubbly-thermal analogy is established on the formal basis. Quite general governing equations for dispersed layers are converted into the equations of thermal layers. In Section 3, experimental results on the stability of bubbly layers are described and compared with the prediction of the theory. In Section 4, a discussion is provided on the similarities and differences between the thermal and two-phase dispersed layers.

UNCORRECTED PROOF

2. Theory

2.1. Physical analogy

2.1.1. Thermal layers

2.1.1.1. Infinite thermal layer. The governing equations in the Boussinesq approximation are (Tritton, 1988):

$$\nabla \cdot \mathbf{v} = 0, \tag{2.1a}$$

$$\rho_0 \left(\frac{\partial \mathbf{v}}{\partial t} + \mathbf{v} \cdot \nabla \mathbf{v} \right) = -\nabla p + \nabla \tau + \rho \mathbf{g}, \tag{2.1b}$$

$$\frac{\partial T}{\partial t} + \mathbf{v} \cdot \nabla T = \kappa \nabla^2 T, \tag{2.1c}$$

where $\boldsymbol{v}$, ρ, g, T, κ are fluid velocity, fluid density, gravity, temperature, heat diffusivity, $\rho = \rho_0(1 - \alpha(T - T_0))$, α is thermal expansivity (subscript 0 denotes a constant reference value). After linearization and scaling, two dimensionless numbers *Ra* and *Pr* appear that describe the layer completely (Drazin and Reid, 1981):

$$Pr \equiv \gamma/\kappa, \tag{2.2}$$

$$Ra \equiv \frac{g\alpha \Delta T H^3}{\gamma \kappa}. \tag{2.3}$$

ΔT is the temperature gradient imposed across the layer and γ is the fluid kinematic viscosity. The neutral equation gives the condition for the onset in terms of the critical value (index c) of the Rayleigh number, $Ra = Ra_c^\infty$, which depends on the boundary conditions (superscript ∞ denotes the horizontally infinite layer). Ra_c^∞ involves the critical temperature gradient ΔT_c and takes the value 658 for slip and 1708 for no-slip boundaries (Drazin and Reid, 1981). The value of Ra_c^∞ contains the complete information about the onset. Although *Pr* does not affect the marginal state, it affects the layer behaviour after the onset. The Nusselt number is introduced for convenience to measure the heat transport through the layer (Tritton, 1988),

$$Nu \equiv J_0/J_1 = (J_1 + J_2)/J_1, \tag{2.4}$$

where J_0, J_1 and J_2 are the total, conductive and convective heat fluxes. *Nu* equals unity before the onset and is larger than unity after the onset, indicating clearly the transition. To determine the onset in experiments, *Nu* is usually plotted against *Ra*, the main control parameter.

2.1.1.2. Finite thermal layer. The Rayleigh number defined by (2.3) with H as the only length scale applies also to layers confined in horizontally finite enclosures. The critical value then depends on the layer width D, the other relevant length scale. It is convenient to express this dependence in the form

$$Ra_c = Ra_c^\infty + f(A), \tag{2.5}$$

UNCORRECTED PROOF

where $f(A)$ is the sidewall correction to the limit value Ra_c^∞ and $A = H/D$ is the layer aspect ratio. The relation (2.5) contains the complete information about the onset in finite containers. Because the lateral walls stabilize the layer, $f(A)$ is a generally increasing function starting from zero and must be found experimentally (Stork and Muller, 1972, 1975). For the idealized slip walls, the approximate theoretical results predict a quadratic leading-order increase, $f \sim A^2$ with different numerical coefficients at A^2 for rectangular and circular containers (Segel, 1969; Brown and Stewartson, 1978). The real data can also be fitted with a power law, see Fig. 1. Note that a two-scale Rayleigh number can be introduced too, by employing a different scaling. This leads to replacing H^3 in (2.3) with HD^2 which is used e.g. at convection in narrow vertical gaps (Edwards, 1969; Hartline and Lister, 1977).

2.1.1.3. Physical meaning of Ra. It follows from the nondimensionalization of (2.1) that *Ra* comprises three ingredients: buoyancy, viscosity, and diffusion. Busse (1978) showed how to define *Ra* physically, in terms of the scale estimates of the relevant forces. Consider a density disturbance within a fluid layer in the form of a warmer and lighter blob, see Fig. 2. If the blob starts rising and passes through the layer, the convective circulation sets in. The buoyancy force on the blob is $F_b \sim g\Delta\rho$. The scale of the density disturbance relates to the scale of the temperature disturbance by $\Delta\rho = \alpha\rho\Delta T$. Here, the temperature difference $\Delta T = T_2 - T_1$ is both the external control parameter (the imposed gradient) and the characteristics of the internal state of the system (the slope of the temperature profile). T_2 is the departure from the state of thermal equilibrium with T_1 The blob temperature decreases due to the heat diffusion in the horizontal direction. Therefore, the buoyancy force must be multiplied by an efficiency factor ζ. The factor is taken as a ratio of two time scales, $\zeta = \tau^H/\tau^V$ the scale of the heat transfer in the horizontal direction τ^H and the scale of the blob rise in the vertical direction τ^V Time τ^H is estimated by H^2/κ, which relates to relaxation of isotherms distorted on the distance H to their steady positions. Time τ^V is estimated by H/v, where v is a velocity scale. Then the buoyancy force is

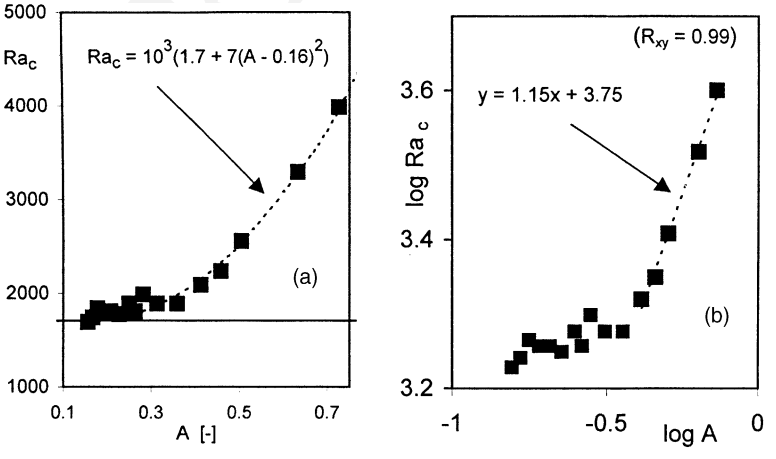

Fig. 1. Thermal layers. Plotting the critical Rayleigh number Ra_c versus layer aspect ratio $A = H/D$ shows the stabilizing effect of sidewalls. (a) Experimental data (marks) allow for the theoretical quadratic fit (dotted line). The origin is shifted since too flat layers seem not to feel the sidewalls. (b) The apparently increasing part of the data (at $A > 0.35$, say) obeys a power law fit (dotted straight line). Data from Stork and Muller (1975).

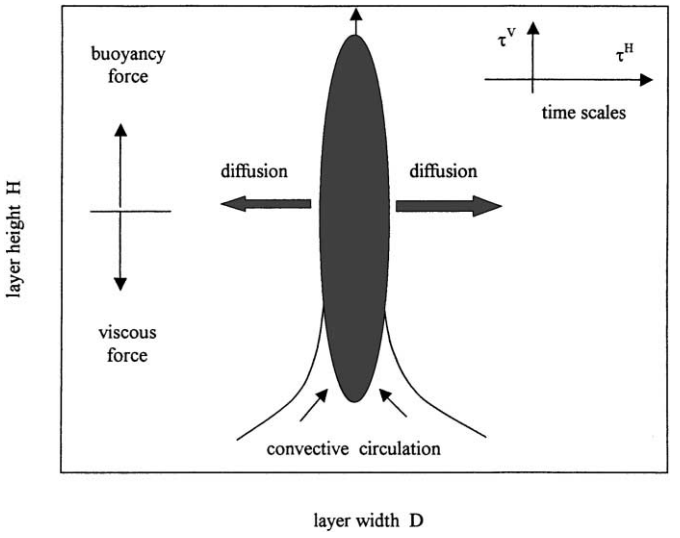

Fig. 2. Buoyant layers. Sketch for defining the Rayleigh number in terms of forces acting on a density disturbance (a light blob) in a uniform buoyant/viscous/diffusive environment.

$$F_b = k_b g\alpha\rho\,\Delta T(vH/\kappa), \tag{2.6}$$

where the unknown proportionality constant k_b depends on the boundary conditions. The scale estimate of the viscous force opposing the blob motion is based on the viscous term of the Navier–Stokes equation and is

$$F_v = k_v\gamma\rho v/H^2, \tag{2.7}$$

where another proportionality constant k_v is used. The Rayleigh number introduced in (2.3) can be alternatively expressed in terms of the forces as

$$Ra \equiv (F_b/F_v)(k_v/k_b). \tag{2.8}$$

This physical definition applies to any buoyant/viscous/diffusive system where the relevant forces can be evaluated. Advantageously, it does not refer to any particular governing equations, which may be unknown or unreliable, especially in case of two-phase flow systems. At the onset, the forces are in balance, $F_b/F_v = 1$, and the critical value is determined by the two proportionality constants that depend on the boundary conditions, $Ra_c = k_v/k_b$ Because Ra_c depends also on the container shape and size (see Eq. (2.5) and below), so do k_v and k_b On the other hand, k_v and k_b do not depend on the properties of the fluid. Note that the two-scale Rayleigh number $\sim HD^2$ results when $\tau^H = H^2/\kappa$ is replaced with $\tau^H = D^2/\kappa$, which is another sensible time scale joined with diffusion.

2.1.2. Dispersed layers (*)

2.1.2.1. Rayleigh number. To introduce the Rayleigh number for dispersed layers, the forces in (2.8) must be evaluated for two-phase mixtures. Consider therefore a buoyant two-phase layer

UNCORRECTED

with the volumetric concentration of the dispersed phase ϕ. Let the basic state of uniform density be disturbed by $\Delta\rho$ on the length scale H, see Fig. 2. Let the disturbance be a positively buoyant blob of a higher concentration of light particles with density $\rho_p < \rho$. If the blob passes through the layer, the convection sets in. The buoyancy force on the blob is $F_b^* \sim g\,\Delta\rho$, where the scale of the density disturbance relates to that of the concentration disturbance by $\Delta\rho = (\rho - \rho_p)\Delta\phi$. Here, $\Delta\phi = \phi_2 - \phi_1$ is the characteristics of the internal state of the system. ϕ_2 is the departure from the state of mechanical equilibrium with $\phi_1 = 0$. It is natural to estimate ϕ_2 by ϕ itself. The particle concentration in the blob decreases due to the gradient hydrodynamic diffusion in the horizontal direction. Therefore the buoyancy force must be multiplied by an efficiency factor ζ^*. The factor is taken as a ratio of two time scales, $\zeta^* = \tau^{H*}/\tau^{V*}$, the scale of the particle transfer in the horizontal direction τ^{H*}, and the scale of the blob rise in the vertical direction τ^{V*}. Time τ^{H*} is estimated by H^2/κ^*, which relates to the relaxation of the concentration profiles distorted on the distance H to the steady state. Time τ^{V*} is estimated by H/v, where v is a velocity scale. Then the buoyancy force is

$$F_b^* = k_b^* g(\rho - \rho_p)\phi(vH/\kappa^*), \tag{2.9}$$

where the unknown proportionality constant k_b^* depends on the boundary conditions. The scale estimate of the viscous force is similar like that in (2.7),

$$F_v^* = k_v^* \gamma^* \rho v / H^2, \tag{2.10}$$

where another proportionality constant k_v^* is employed and γ^* denotes the effective viscosity of the mixture. On the basis of (2.8), the Rayleigh number of dispersed layers is defined as

$$Ra^* \equiv (F_b^*/F_v^*)(k_v^*/k_b^*) = \frac{g'\phi H^3}{\gamma^*\kappa^*}, \tag{2.11}$$

where g' is the reduced gravity $g|\rho - \rho_p|/\rho$. At the onset, the forces are in balance, $F_b^*/F_v^* = 1$, and the critical value is determined by the boundary conditions via the proportionality constants, $Ra_c = k_v^*/k_b^*$. Besides the container shape and size, k_v^* and k_b^* may potentially depend on certain parameters of the two-phase mixture. By the analogy, a similar stabilizing effect of the sidewalls is anticipated for the dispersed layers and the counterpart of (2.5) is the following formula:

$$Ra_c^* = Ra_c^{\infty *} + f^*(A), \tag{2.12}$$

which must be found experimentally by plotting the values of the critical Rayleigh number $g'\phi_c H^3/\gamma^*\kappa^*$ against the layer aspect ratio A. The relation (2.12) contains the complete information about the onset. Note that the dispersed two-scale Rayleigh number $\sim HD^2$ results when $\tau^{H*} = H^2/\kappa^*$ is replaced with $\tau^H = D^2/\kappa^*$, which is another sensible time scale joined with diffusion.

2.1.2.2. Stability criterion. The stability condition can be expressed either in terms of the critical Rayleigh number, $Ra^* < Ra_c^*$, see (2.12), or, equivalently, by mere rearranging (2.12), in terms of the critical voidage, which is a more convenient quantity,

$$\phi < \phi_c = \frac{\gamma^*\kappa^*}{g'}\,\frac{Ra_c^{\infty *} + f^*(A)}{H^3}. \tag{2.13}$$

UNCORRECTED PROOF

This is the main result of the study. It should apply quite generally to dispersed layers governed by buoyancy, viscosity, and diffusion. The value of the critical voidage ϕ_c is the measure of the homogeneous layer stability. Obviously, the higher the critical voidage ϕ_c the more stable the layer. In (2.13), the limit value $Ra_c^{\infty *}$ is a numerical parameter and the wall correction function $f^*(A)$ is a functional parameter of the theory. Numerical values of these two parameters must be determined experimentally.

2.1.2.3. Prandtl and Nusselt numbers. The Prandtl number for dispersed layers is defined in accord with its thermal counterpart (2.2) as

$$Pr^* \equiv \gamma^*/\kappa^*. \tag{2.14}$$

It measures the relative importance of viscosity and diffusion in two-phase mixtures and depends on the mixture properties. The Nusselt number is defined in accord with (2.4) as

$$Nu^* \equiv J_0^*/J_1^* = (J_1^* + J_2^*)/J_1^*, \tag{2.15}$$

where J_0^*, J_1^*, and J_2^* are the total, conductive, and convective fluxes of the dispersed phase through the layer. The onset of convection is indicated by the departure of Nu^* from unity in the plot of Nu^* versus Ra^*. In bubble columns, the total buoyancy flux J_0^* equals the superficial gas velocity $q = Q/S$, where Q is the volumetric gas flow and S the cross-section area. The homogeneous–heterogeneous regime transition is a gradual process and the conductive and convective fluxes can be expressed as $J_1^* = (1-\beta)q$ and $J_2^* = \beta q$, where β is the fraction of the column occupied by the heterogeneous regime (indexes 1 and 2 refer to homogeneous and heterogeneous regimes respectively). Relation (2.15) then simplifies to

$$Nu^* = 1/(1-\beta). \tag{2.16}$$

As an example, to demonstrate how the onset can be determined from experimental data, Nu^* is plotted against Ra^* in Fig. 3. The data are taken from our previous measurements in bubble columns, where the values of β were determined (Ruzicka et al., 2001a). It is convenient to express the scale of the voidage disturbance ϕ in the definition (2.11) by $\phi = q/u$, which is the mass

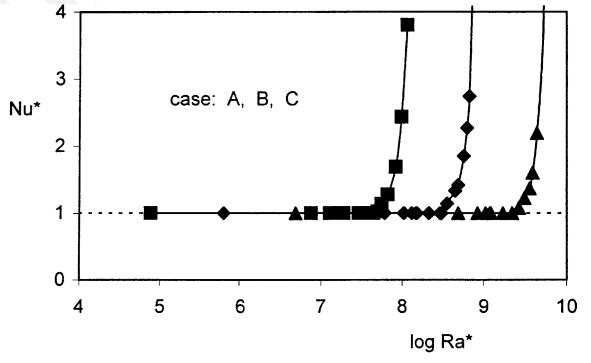

Fig. 3. Bubbly layers. Plotting the bubbly Nusselt number Nu^* versus the bubbly Rayleigh number Ra^* indicates the onset of convection in bubbly layers. Experimental data (connected marks) from Ruzicka et al. (2001a). ($D = 0.15$ m; $H = 0.25$ m (case A), $H = 0.5$ m (case B), $H = 1$ m (case C)).

conservation equation of the gas phase in the uniform steady state of the column. q is the main control parameter of the experiment, the buoyant energy input. u is the mean gas phase rise velocity (at zero net liquid flux also mean bubble slip speed), whose scale estimate is the terminal bubble rise velocity w. Further, considering $g' \approx g$ for the water–air system and taking $\gamma^* \approx \gamma$, the bubbly Ra^* becomes $gqH^3/w\gamma\kappa^*$, which is used in the plot in Fig. 3.

2.2. Formal analogy

So far, only the physical analogy between the two systems has been pursued. In this section, the conditions are specified, under which the governing equations of the thermal and dispersed layers are formally similar in the case of 1D dispersed flows. The fundamental equations (2.1) of thermal layers are widely accepted (Drazin and Reid, 1981; Tritton, 1988; Koschmieder, 1993). On the other hand, there is much less consensus on numerous equations suggested for two-phase mixtures. They lack the fundamental basis due to the complexity of two-phase flows (Minev et al., 1999; Jackson, 2000). The equations for the *fluid phase* are easier to formulate. They are acceptable in the form

$$\rho_0 \frac{\partial}{\partial t}(1-\phi) + \rho_0 \nabla((1-\phi)\mathbf{v}) = 0, \tag{2.17a}$$

$$\rho_0(1-\phi)\left(\frac{\partial \mathbf{v}}{\partial \mathrm{t}} + \mathbf{v}\cdot\nabla\mathbf{v}\right) = -(1-\phi)\nabla p + \nabla\tau^* \rho_0(1-\phi)\mathbf{g} + \mathbf{F}. \tag{2.17b}$$

Unlike its thermal counterpart (2.1a), the continuity equation (2.17a) is 'compressible' due to the variable void fraction. The dispersed momentum equation (2.17b) differs from the thermal momentum equation (2.1b) by a more complicated stress tensor and by the phase interaction force $\mathbf{F}$. The equations for the *dispersed phase* present a great difficulty. Considerable progress has recently been made in formulating these equations for 1D flows. Batchelor (1988) derived his equations from the first principles. Biesheuvel and Gorissen (1990) obtained their equations using an averaging procedure in a similar form as Batchelor. These equations contain all relevant physical phenomena whose importance has yet been recognized and were successfully tested experimentally (Lammers and Biesheuvel, 1996). They are of the following general form (Batchelor, 1988):

$$\frac{\partial \phi}{\partial \mathrm{t}} + \frac{\partial}{\partial x}(\phi u) = 0 \quad \text{(mass)}, \tag{2.18a}$$

$$\text{(acceleration)} + \text{(elasticity)} + \text{(particle stress)} = \text{(buoyancy)} + \text{(drag)} + \text{(diffusion)} \quad \text{(momentum)}. \tag{2.18b}$$

In the dynamic equation (2.18b), the inertial terms are located on the left-hand side and the noninertial terms are on the right-hand side.

The difference between the governing equations of the buoyant agent in thermal and dispersed layers is substantial. It is seen from comparing the one heat equation (2.1c) with the two dispersed phase equations (2.18a) and (2.18b). However, (2.18a) and (2.18b) can be converted into (2.1c) provided that the particle (bubble) inertia and particle (bubble) slip speed are negligible—this is called the *thermal limit* of dispersed layers. We follow the procedure by Batchelor (1988) for extracting the kinematic mode from his equations. The linearized dimensionless equations of the

UNCORRECTED PROOF

dispersed phase (2.18) for small departures from uniformity (index 0) in a reference frame travelling with the mean mixture velocity U are (Batchelor, 1988):

$$\phi_t + \phi_x + \phi_0 u_x = 0 \quad \text{(mass)}, \tag{2.19a}$$

$$A_1(u_t + u_x) - A_2 u_x - A_3 u_{xx} + A_4 \phi_x = \psi(A_5\phi - A_6 u - A_7\phi_x) \quad \text{(momentum)}. \tag{2.19b}$$

The coefficients $A_{1\text{–}7}$ generally depend on ϕ, U, the particle Reynolds number, and the particle–fluid density ratio ρ_p/ρ. Their physical meaning is as follows: $A_{1,2}$—added mass, A_3—particle viscosity, A_4—bulk modulus of elasticity, A_5—density, A_6—friction, A_7—hydrodynamic diffusivity. CoefficientsA_4 and A_7 play an important stabilizing role. The parameter ψ has the meaning of the Richardson number, i.e. (Froude number)$^{-2}$. u is the bubble velocity relative to U. This drift velocity u is simply related to the slip velocity u_s by $u = (1-\phi)u_s$. Neglecting the inertia terms by putting $\psi \to \infty$ and substituting for the coefficients ($A_5 = \phi_0 u_0'$, $u_0' = (\mathrm{d}u/\mathrm{d}\phi)_0$, $A_6 = \phi_0$, $A_7 = \kappa^*$), Eq. (2.19b) becomes $\phi_0 u = -\phi_0 u_0' \phi - \kappa\phi_x$ Taking the derivative d/dx of this equations, substituting for $\phi_0 u_x$ into (2.19a), and expressing it in the dimensional variables in the laboratory reference frame gives

$$\phi_t + (U + u_0 + \phi_0 u_0')\phi_x = \kappa^* \phi_{xx} \quad \text{(mass + momentum)}. \tag{2.20}$$

If the slip speed is zero, $u_s \equiv 0$, so are u_0 and u_0' and only $U\phi_x$ remains from the round bracket. The mixture velocity U then becomes the fluid velocity v. Under these conditions, (2.20) reads

$$\phi_t + v\phi_x = \kappa^* \phi_{xx} \quad \text{(mass + momentum)}, \tag{2.21}$$

which is the 1D analogue of the heat equation (2.1c). The bubbly-thermal analogy is thus proved on the level of the governing equations. The condition of zero slip speed corresponds to a neutrally buoyant agent and implies $\rho_p \approx \rho$. This makes the interaction force $\mathbf{F}$ in (2.17b) zero, because it is usually taken proportional to the slip speed and/or the density difference $(\rho - \rho_p)$. For instance, Shnip et al. (1992) used $\mathbf{F} = (1-\phi)\phi(\rho - \rho_p)g$. With $F = 0$, Eq. (2.17b) is closer to its thermal counterpart (2.1b).

3. Experiment

The theory presented in this paper is a physical scaling theory, which is based on scale estimates of the forces that control the evolution of a density disturbance in a uniform buoyant layer. The theory contains two parameters, namely $Ra_c^{\infty *}$ and $f^*(A)$, whose numerical values must be determined from experimental data. Therefore, an extensive set of experiments with bubbly layers in bubble columns was performed to establish (2.12) and to verify (2.13). The experiments were focused on the effect of the column size on the homogeneous regime stability, which is important for the scale-up and design of real reactors. Because of their relevance for the chemical engineering community, the results have already been published in a separate paper (Ruzicka et al., 2001b) and are only briefly discussed here.

In our experiments (Ruzicka et al., 2001b), three cylindrical bubble columns with diameters $D = 0.14$, 0.29, 0.40 m were used and the ungased layer height H varied from 0.1 to 1.3 m, giving the aspect ratio A from 0.71 to 9.3. Compressed air and tap water were used as the phases. The gas passed through a 3-mm thick perforated brass plate with small, precisely drilled, circular orifices

UNCORRECTED PROOF

0.5 mm in diameter arranged in a regular hexagonal lattice with 10 mm pitch and the relative free plate area 0.2 %. Under these conditions, fairly uniform bubbly layers are produced (Kastanek et al., 1993). The dependence of the voidage ϕ (calculated from the layer expansion) on the superficial gas velocity q (measured by rotametres) was obtained with a relative error less than 5%. To determine the critical point $[q_c, \phi_c]$, the primary data $\phi(q)$ were re-plotted according to the drift-flux concept (Wallis, 1969) in the coordinates the drift-flux j and the voidage ϕ. The onset was indicated by the departure of the experimental data $j = (1 - \phi)q$ from the theoretical curve $j = \phi(1 - \phi)u$, where u is bubble slip speed. Instead of one of many empirical formulas for $u(\phi)$ suggested mostly for sedimenting systems (e.g. Richardson and Zaki, 1954), we used a nonempirical expression derived for uniform bubbly layers (Ruzicka et al., 2001a),

$$u(\phi) = w\left(1 - \frac{a\phi}{1-\phi}\right). \tag{3.1}$$

The values of the parameters w (terminal bubble velocity) and a (bubble drift coefficient) were determined from the experimental data by linearizing (3.1). Knowing the critical voidage ϕ_c the corresponding critical Rayleigh number was calculated by (2.11). The viscosity of the bubbly mixture was approximated by that of water, $\gamma^* \approx \gamma = 10^{-6}$ m^2/s. The hydrodynamic bubble diffusivity was estimated as suggested by Batchelor (1988), $\kappa^* \approx dw$, where d is the bubble diameter. For our bubbles, $d \approx 0.005$ m and $w \approx 0.2$ m/s giving $\kappa^* \approx 10^{-3}$ m^2/s.

To establish the relation (2.12), Ra_c^* was plotted against A and a good power-law fit of the experimental data was found in a general form (Ruzicka et al., 2001b):

$$Ra_c^* = Ra_c^{\infty *} + f^*(A) = k_1 + k_2 A^c, \tag{3.2}$$

in particular,

$$Ra_c^* \approx 10^5 + 6.70 \times 10^6\ A^{2.84} \quad (D = 0.14\ \text{m}),$$
$$Ra_c^* \approx 10^5 + 4.72 \times 10^7\ A^{2.80} \quad (D = 0.29\ \text{m}),$$
$$Ra_c^* \approx 10^5 + 1.12 \times 10^8\ A^{2.74} \quad (D = 0.40\ \text{m}).$$

With help of (3.2), the stability condition (2.13) for our bubbly layers can be written as

$$\phi < \phi_c = \frac{\gamma^* \kappa^*}{g'}\left(\frac{k_1}{H^3} + \frac{k_2}{H^{3-c} D^c}\right), \tag{3.3}$$

where $k_1 \approx 10^5$ is the critical Rayleigh number of the horizontally infinite layers, k_2 is the coefficient of the correction function, by 2–3 orders of magnitude larger than k_1 and c is the exponent of the power-law correction function with values between 2.5 and 3, say. The critical voidage predicted by (3.3) compares well with the experimental data (Ruzicka et al., 2001b) (see Fig. 4). Considering the simplicity of the present scaling theory, the agreement is very good.

4. Discussion

The crucial difference between the dispersed and thermal layers is that, unlike heat, the dispersed particles are physical individual, moving relatively to the fluid with their own inertia and

UNCORRECTED PROOF

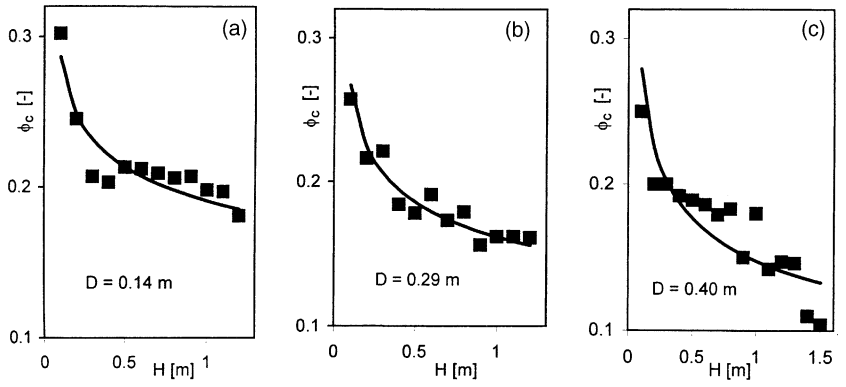

Fig. 4. Bubbly layers. Effect of the container width on the critical voidage: comparison of the present theory (stability criterion (3.3), lines) with the experimental data (marks) from Ruzicka et al. (2001b).

undergoing interactions. It has two consequences for the *basic state*: the presence of the small-scale flow field and the absence of the vertical density gradient. In the case of bubbles, the background flow field is produced by the coherent upwelling effect due to the Darwinian drift (e.g. Eames et al., 1994) of the collectively rising bubbles. Fortunately, this coherency is lost by the passage of the backflow through the pseudo-random bed of fluctuating bubbles. The uniformity is thus recovered in the statistical sense on longer time scales and the basic state can be defined as the long-term rest. Heat needs a gradient to move through a stagnant layer and diffusion is the only mean of the transport. Dispersed particles have two transport mechanisms: hydrodynamic diffusion and free rise, both of comparable rates. Indeed, the time scale of the former is $d^2\kappa^* \sim d^2/dw \sim d/w$ and that of the latter is d/w. Particles endowed with the ability of active motion do not wait till a stable diffusion profile is developed. Fortunately, the density profile is not essential for the convective instability to occur. It suffices to have a mechanism that produces voidage disturbances in a uniform layer. This is ensured by the hydrodynamic interactions among the particles and between them and the background flow field. In case of zero relative motion between the phases, the background field vanishes and the particles develop the linear diffusion profile.

In thermal layers, the *onset* is a sudden supercritical event, provided that the boundaries are perfectly conducting or insulating. The thermal onset can be made gradual by imperfect walls, where small subcritical motions exist and the onset goes via an imperfect bifurcation (Koschmieder, 1993). On the other hand, the onset in dispersed layers is a continuous process of a gradual increase in the population of coherent structures living in the background flow field. By suppressing this background field, the onset will be sudden too.

The *first mode* after the onset in thermal layers, the convective cells, is well-defined, temporally steady, spatially regular, and linearly stable. In dispersed layers, the convective motions are ill-defined, highly unsteady, spatially irregular, random, and their stability is difficult to assess. Only after taking the long-term average, these motions display smooth and steady circulation loops similar to the thermal cells.

It follows that even the thermal and dispersed layers differ from one another in several aspects, these differences are, however, not fatal. Moreover, the differences can be removed by employing

long-term view at the dispersed layers and letting the relative motion between the phases become negligible. Under these conditions, both layers are physically similar and are expected to display identical behaviour near the onset of convection.

On the grounds of the above *physical* similarities between the thermal and dispersed layers, it is tempting to make a link between these two. A simple way is to introduce the Rayleigh, Prandtl, and Nusselt numbers for the dispersed layers.

The dispersed *Rayleigh number* (2.11) was introduced on physical grounds in terms of forces following the Busse's (1978) reasoning. From (2.3) and (2.11) we can see that the thermal buoyancy factor $\alpha\Delta T$ is replaced with ϕ, the heat diffusivity with the hydrodynamic diffusivity κ^*, and the gravity g with g'. Comparing the thermal and bubbly buoyant effects, $\alpha\Delta T$ and ϕ, it can be shown readily that one cubic metre of air in water gives the same buoyant effect as 2.8×10^{10} Joules of heat. One 5-mm bubble then represents about 1800 J. Unfortunately, the theory of the hydrodynamic diffusion at the intermediate Reynolds number is far from being developed (Davis, 1996). The gradient diffusion is a complex process where a macroscopic flux of the dispersed phase is generated by complicated hydrodynamic interactions between a large number of individual dispersed particles. Due to the interactions, a particle experiences larger total force from the side with more neighbours. As a result, it moves into a region with a lower particle concentration, i.e. down the concentration gradient. Because of lack of anything better, we are on mercy of simple scale estimates for the diffusivity, like $\kappa^* \sim dw$ (see e.g. Batchelor, 1988 and Batchelor and Nitsche, 1991). For thermal convection in water layers and two-phase convection in water–air bubbly layers, it is $g\alpha/(\gamma\kappa) \approx g'/(\gamma^*\kappa^*) \approx 10^{10}$ giving thus $Ra \approx 10^{10}\,\Delta T H^3$ and $Ra^* \approx 10^{10}\,\phi H^3$ Because the product $\Delta T H^3$ is usually much smaller than ϕH^3 the dispersed Ra^* is expected to be much larger than the thermal Ra, which is $\sim 10^3$ near the onset. Indeed, Ra^* in the range 10^4–10^{10} was found in our experiments with bubbles, and the limit value was estimated $Ra_c^{\infty *} \approx 10^5$, see relations (3.2) and Ruzicka et al. (2001b). Other authors reported similar values of the dispersed Rayleigh number. Rothman and Kadanoff (1994) found $Ra^* \sim 10^7$ typical for bubbles and Tong and Ackerson (1998) estimated $Ra^* \sim 8.8 \times 10^7$ typical for sedimenting layers. Kimura and Iga (1995) used Ra^* of 10^4–10^{10} in 2D simulations and had $Ra^* = 2.5 \times 10^5$ in 2D experiments. Climent and Magnaudet (1999) obtained $Ra_c^* \approx 2.2 \times 10^5$ from 2D simulations. Note, however, that Kimura and Iga and Climent and Magnaudet did not consider the hydrodynamic diffusion. Kimura and Iga obtained $Ra^* = g'qH^2/\gamma w^2$ by scaling the two-phase governing equations where the inertial estimate Hw based on the bubble slip speed w stands in place of the hydrodynamic diffusivity $\kappa^* \sim dw$. Climent and Magnaudet introduced the bubbly number as $Ra^* = g\phi H^2/\gamma w$, which relates to that of Kimura and Iga by the continuity relation $\phi = q/w$ (see below the Eq. (2.16)). Because all these authors had $H \sim 10^3 d$, their inertial estimate Hw is by three orders of magnitude larger than the diffusivity $\sim dw$, so that their inertia-based Ra^* is also by three orders of magnitude larger than the diffusion-based Ra^*.

The dispersed *Prandtl number* was introduced in (2.14) purely formally to retain the physical meaning of its thermal counterpart (2.2). Both γ^* and κ^* represent the constitutive properties of the two-phase mixture and are difficult to evaluate precisely (Kang et al., 1997; Tory, 2000). For our bubbles ($\gamma = 10^{-6}$ m^2/s, $d = 5 \times 10^{-3}$ m, $w = 0.2$ m/s) with the large Reynolds number $Re = dw/\gamma = 10^3$, the diffusion-based Prandtl number is estimated as $Pr^* = \gamma^*/\kappa^* \approx \gamma/\kappa^* \sim \gamma/dw = 10^{-3}$. Note that Pr^* evaluated this way equals $1/Re$. If, however, the effective mixture viscosity is estimated by scales as $\gamma^* \sim dw$, and the diffusivity as $\kappa^* \sim dw$ too, then $\gamma^* \sim \kappa^*$ and the

dispersed Pr^* is a constant (of order of unity?). Tong and Ackerson (1998) estimated $Pr^* \approx 3.8 \times 10^3$ from previous experimental data on Stokes suspensions with small Re. Kimura and Iga (1995) obtained the inertia-based bubbly Prandtl number by scaling the diffusionless governing equations, $Pr^* = \gamma/Hw$, with values $Pr^* \sim 10^{-3} - 10^1$ in simulations and $Pr^* \sim 3 \times 10^{-2}$ in experiments. For their bubbles ($\gamma = 10^{-6}$ m^2/s, $d = 2.5 \times 10^{-5}$ m, $w = 3.6 \times 10^{-4}$ m/s) with $Re = 9 \times 10^{-3}$, the diffusion-based $Pr^* = \gamma\kappa^*$ equals 111. Climent and Magnaudet (1999) used the same inertial-based $Pr^* = \gamma/Hw$ and kept it constant, $Pr^* = 2.5 \times 10^{-4}$. Their bubbles had $Re \approx 4$ (at $\gamma = 10^{-6}$ m^2/s, $d = 2 \times 10^{-4}$ m, $w = 2 \times 10 - 2$ m/s) and therefore the diffusion-based $Pr^* = \gamma^*/\kappa^*$ is $\approx$0.25.

The dispersed *Nusselt number* Nu^* was introduced in (2.15) purely formally to retain the physical meaning of its thermal counterpart (2.4). Replacing the conductive and convective heat fluxes in (2.4) with the corresponding mass fluxes of the buoyant phase is the obvious choice. The definition (2.15) simplifies to (2.16), if the transition to the convective regime is gradual.

Note that the convection in bubbly layers studied by Kimura and Iga (1995) and Climent and Magnaudet (1999) was triggered by the Rayleigh–Taylor instability, where no wavelength selection occurs, rather than by the Rayleigh–Benard instability, where the opposite is true. Therefore, their and our results do not correspond completely. For instance, the 'critical' Rayleigh number in these studies refers to the state where the layer is unable to develop into steady circulation cells, i.e. it refers to the results of the layer time evolution rather than to a property of the uniform basic state. For instance, Kimura and Iga (1995) found that the layer develops into steady cells only at low Pr^*, that the value of critical Ra_c^* increases with Pr^*, that the cell aspect ratio A is typically larger than 1, and that the cell size increases with Ra_c^*.

Regarding the stability criterion (2.13), we believe that, if the analogy is perfect, the values of $Ra_c^{\infty *}$ and $f^*(A)$ are universal and (2.13) is fully predictive. As with the thermal layers, the critical value $Ra_c^* = k_v^*/k_b^*$ should depend only on the boundary conditions and the container geometry. However, we suspect that real bubbly layers in real columns may violate the wistful perfectness and k_v^* and k_b^* may depend also on properties of the two-phase mixture, e.g. on the bubble size.

To obtain the analogy on the *formal* level means to specify the conditions, under which the thermal and dispersed governing equations become equivalent. One way is to reduce the dispersed equations, while the other is to extend the thermal equations.

In Section 2.2, a particular set of dispersed equations (2.17)–(2.18) in a particular case of 1D flow was reduced to the thermal equations (2.1) under the condition of negligible particle inertia and slip speed. We believe that a similar procedure will work also for other sets of governing equations, and in 2D and 3D. If the particle *inertia* is neglected in the linearized momentum equation (2.19b) by putting the left-hand side zero, the right-hand side describes the dynamical balance (equilibrium) between two momentum fluxes into a control element: (buoyancy) − (drag) = (diffusion). Taking the derivative d/dx of this balance gives the expression of the quantity $\phi_0 u_x = \phi_0 u_0' \phi_x - \kappa^* \phi_{xx}$ which is the convective contribution to the mass flux generated by the equilibrium dynamics and driven by the local velocity gradientu_x This expression is substituted into the mass equation (2.19a) yielding (2.20), which then remains the only governing equation of the dispersed phase. Under these conditions, the hydrodynamic diffusion, which essentially is a dynamic process of the momentum exchange due to the inter-bubble repulsive forces, becomes a kinematic process, as stressed by Batchelor (1988). The buoyancy-to-inertia parameter $\psi = \sigma g' L/U^2$ in (2.18b) relates to the Richardson number $Ri = g'L/U^2$. σ is a

nearly constant number and L is the disturbance wavelength, as a length scale. Long wave disturbances ($\psi \to \infty$) are governed by the kinematic mode. Biesheuvel and Gorissen (1990) interpret ψ equivalently, as a ratio of inertia-to-viscous relaxation times: the stronger the force, the shorter the time. Another kind of merger of the momentum and mass equations is known from interactions between dynamic and kinematic waves (e.g. Wallis, 1969). The linearized continuity equation (2.21) supports kinematic concentration waves with speed ($U + u_0 + \phi_0 u_0'$) damped by $\exp(-\kappa^* k^2 t)$, k is the wavenumber: the shorter the wave, the stronger the damping. $\phi_0 u_0'$ is the relative speed between the wave and the particles, u_0' between the particles and the mixture, and U between the mixture and the laboratory. If the relative motion of the phases is negligible, i.e. the *slip speed* tends to zero, then the drift velocity u_0 and its derivative u_0 tend to zero too. The dispersion then supports waves relative to neither the particles nor the mixture, which further stabilizes the homogeneous state. Beyond linearization, the continuity equation (2.18a) equipped with the diffusion term is the Burgers equation (Whitham, 1974). The nonlinear amplitude steepening due to the change of the slip speed with the voidage is opposed by diffusion. Note that both the decrease of the slip speed due to the hindrance effect (Davis and Birdsell, 1996; Brenner, 1999) and the increase due to the shielding effect (Yuan and Prosperetti, 1994; Ruzicka, 2000) are possible. As a result, stable wave profiles may develop. Burgers' waves in bubbly flows were studied by Lammers and Biesheuvel (1996).

Regarding the other way, the extension of the thermal equations, we expect that it can be done by a suitable perturbation expansion of the set (2.1). The dynamic equation for the buoyant agent will have to be constructed anew, which may be a difficult task to do it rigorously, at least due to the apparent ambiguity of the problem.

We lack systematic *experiments* focused on the convective instability of dispersed layers. Those by Agarwal et al. (1980) were aimed at the verification of the former theory developed for fluidized bed (Medlin et al., 1974). The results obtained in a flat column (thickness 1.9 cm) proved the theory predictions: bed stabilization by decreasing column width and increasing column height, the later being in contradiction with our data. The reason may be seen in the two-dimensionality of the problem, considered in the theory and reflected in the experiments. The measurements by Kimura and Iga (1995) performed with very small bubbles close to the thermal limit, i.e. low inertia ($Re = 9 \times 10^{-3}$) and slip speed ($w = 3.6 \times 10^{-4}$ m/s), were rather qualitative (only visualization) and of poor reproducibility. Although they were aimed at finding the Rayleigh–Benard instability in bubbly layers, they actually led to the Rayleigh–Taylor instability. The latter basically refers to the interfacial instability of two immiscible fluids superposed in the top-heavy arrangement (Drazin and Reid, 1981). When the originally horizontal interface is disturbed, a region of the light fluid gets into the heavier fluid, and vice versa. The buoyancy force tends to increase the mutual penetration, while the interphase tension force tends to oppose it. The final outcome depends on the relative size of these forces. This concept can be transferred to dispersed layers. Here, the horizontal interphase is the front between two regions of high and low particle concentration. Because these regions are not immiscible, there is no interfacial tension and its stabilizing effect must be produced by a different physical mechanism. It is not clear what mechanism can be operating here. In the particular case of the rising interphase between the clear liquid and the bubbly mixture beneath it in an early period of sparging, the dependence of the bubble slip speed on the local bubble concentration and the bubble arrangement seems to play a certain role. The Rayleigh–Taylor instability of the interphase between dense and sparse regions

in a fluidized bed was studied (Didwania and Homsy, 1981). It was found that the interphase stability strongly depends on the uniformity of the both regions. Therefore, the instability observed by Kimura and Iga (1995) may well be due to violating the condition of the primary homogeneity. To produce homogeneous layers, the bubbles must be not only uniformly but also *densely* packed. The homogeneity results from extremely strong bubble–bubble interactions that are kept short-range by the close packing. This is often misunderstood and the homogeneous regime is referred to as to one where the interactions are absent. The bubble spacing should be comparable with the bubble size d. The horizontal bubble spacing is given by the orifice pitch p. The ratio p/d is a measure of the horizontal heterogeneity of the primary voidage distribution and takes a large value in the experiments of Kimura and Iga, $p/d = 40$. This is directly responsible for the formation of separated bubble chains instead of uniform bubbly layers. Under these circumstances, the Rayleigh–Taylor instability naturally occurs. Another consequence of the large pitch is a low voidage, less than 1% in Kimura and Iga. For comparison, in our experiments $p/d = 2$ and the voidage was up to 50%.

There is a large amount of experimental data produced by chemical engineers on the homogeneous–heterogeneous regime transition in bubble columns, which is interpreted here as the onset of convection. However, detailed and consistent measurements where the critical point is precisely evaluated and the critical values plotted against important control parameters are absent. Instead, many partial and often controversial results are scattered in the literature. Therefore, we started an extensive experimental campaign to investigate effects of operating parameters on the regime transition and to validate the theoretical result (2.13), namely the effects of H, D, γ, and possibly κ^*.

The experiments on the effects of the container size H and D have been completed and the results published (Ruzicka et al., 2001b). The experimental relations (3.2) show that the sidewall correction can be expressed by a power law function. The same expression applies also to the thermal data, see Fig. 1b. While the limit value $Ra_c^{\infty *} \sim 10^5$ in (3.2) applies to all the data, the parameters k_2 and c vary with the container width D. The reason is likely that our bubbles ($Re \sim 10^3$) were far from the thermal limit. We expect that approaching the limit, k_2 and c will converge to universal values. The prediction of the theory (3.3) agrees well with the experimental data (see Fig. 4). The criterion (3.3) predicts a considerable decrease of the stability with increasing the column size in both the vertical and horizontal directions. The first term $\sim 1/H^3$ in the bracket of (3.3) belongs to the horizontally infinite layer and the additional second term $\sim 1/H^{3-c}D^c$ expresses the stabilizing effect of the sidewalls. For the infinite layer, the dimension H appears to the third power, which is the volume of the elementary convective cell, $\phi_c \sim 1/$(cell volume). The volume relates to the number N of dynamic degrees of freedom by the classical Landau argument (Landau and Lifshitz, 1997), $N \sim$ (system volume/smallest eddy volume), hence $\phi_c \sim 1/N$, where the smallest eddy size is the Kolmogorov scale. The stability condition obtained previously by Shnip et al. (1992) also predicts the destabilizing effect of the column size and was compared with our data with a relative success (Ruzicka et al., 2001a,b). The relation (3.3) predicts $\phi_c > 1$ for very small H and D, which is unrealistic. To obtain the voidage less than unity, the dimensions must obey $H > k_1\gamma^*\kappa^*/g'$ and $D > k_2\gamma^*\kappa^*H^{c-3}g')^{1/c}$ For our parameter values, it gives roughly $H > 0.02$ m and $D > 0.08H^{1-3/c} \approx 0.1$ m for $H = 0.02$ m.

The experiments on the effect of the liquid viscosity γ are currently under way. Despite the general experience that the viscosity destabilizes the homogeneous regime and advances the re-

gime transition, our recent measurements indicate that it can also delay the transition and stabilize the uniform basic state. This would be in accord with the prediction of our theory: $\phi_c \sim \gamma^* \approx \gamma$, see (2.13). The stabilizing effect of the diffusivity $\phi_c \sim \kappa^*$ predicted by (2.13) is difficult to investigate because we need more information about the process of the hydrodynamic diffusion. The relation (2.13) also predicts $\phi_c \sim 1/g'$, where $g' = g|\rho - \rho_p|\rho$. Therefore, dispersed layers should be more stable (large ϕ_c) under microgravity conditions (small g) and at low interphase density difference (small $|\rho - \rho_p|$).

Detailed experiments with bubbly layers have to be carried out to verify various aspects of the analogy. For instance, it is expected that decreasing the bubble size from millimetres (perforated plates) to microns (electrochemically generated bubbles), a sudden onset of the steady circulation cells will be observed. We plan to do this work in near future.

Note that the physical analogy (Section 2.1) works well (Fig. 4) even with relatively large bubbles ($\sim$5 mm) at the price of varying k_2 and c. This indicates that the present scaling theory is robust with respect to the details of the microdynamics. On the other hand, the formal analogy (Section 2.2) strictly insists on the negligible bubble inertia and bubble slip speed and is therefore much more restrictive than the physical analogy. Experiments with very fine bubbles are needed to reach the thermal limit. In this respect, the results on plumes of microbubbles obtained recently by Chen and Cardoso (2000) and Climent (2001) are highly encouraging: the scaling for bubble plumes seems to approach that of the thermal plumes.

Although the analogy was developed with bubbly layers in mind, it should also apply to other flow systems where uniform layers of dispersed particles are encountered, both man-made and natural, e.g. industrial sedimentation, fluidized beds, populations of gas bubbles released in oceans, fine solids settling in natural gravity currents and pyroclastic flows, layers of raindrops, etc.

5. Conclusions

A simple physical theory is suggested for the analogy between the onset of convective motions in thermal and bubbly layers. The Rayleigh, Prandtl and Nusselt numbers are introduced for bubbly layers. The stability criterion for the onset is obtained on the basis of the critical bubbly Rayleigh number. The theoretical predictions are in general agreement with experiments. It is also shown how to obtain a formal similarity between the governing equations of the bubbly and thermal layers.

Acknowledgements

MCR would like to thank The Royal Society of London for awarding the postdoctoral fellowship supervised by Prof. N.H. Thomas, where the ideas developed in this study originated (see our report: *Bubbly flows, fluidized beds, and thermal convection*, University of Birmingham, Birmingham, UK, 1995). A part of the work was done during the MCR's visit at the Department of Applied Mathematics and Theoretical Physics (DAMTP) and at the Institute of Theoretical Geophysics (ITG), University of Cambridge, Cambridge, UK, thanks to Prof. H.E. Huppert. The

UNCORRECTED PROOF

authors would like to thank Prof. H.E. Huppert and Dr. J.R. Lister (ITG/DAMTP) for reading the manuscript and useful comments. MCR would like to thank Dr. J. Magnaudet (Institute of Fluid Mechanics, Toulouse, France) and Dr. E. Climent (Institute of Fluid Mechanics, Strasbourg, France) for helpful discussions. The support from the Grant Agency of the Czech Republic (no. 104/01/0547) and the CEC Inco-Copernicus Project by the EC (no. ERB IC15-CT98-0904) is gratefully acknowledged. The present work has been announced at the *4th International Conference on Multiphase Flow* (New Orleans, USA, 2001) and at the *Euromech Colloquium no. 421* (Grenoble, France, 2001).

References

Agarwal, G.P., Hudson, J.L., Jackson, R., 1980. Fluid mechanical description of fluidized beds. Experimental investigation of convective instabilities in bounded bed. Ind. Eng. Chem. Fund. 19, 59–66.

Batchelor, G.K., 1988. A new theory of the instability of a uniform fluidized bed. J. Fluid Mech. 193, 75–110.

Batchelor, G.K., Nitsche, J.M., 1991. Instability of stationary unbounded fluid. J. Fluid Mech. 227, 357–391.

Batchelor, G.K., Nitsche, J.M., 1993. Instability of stratified fluid in a vertical cylinder. J. Fluid Mech. 252, 419–448.

Biesheuvel, A., Gorissen, W.C.M., 1990. Void fraction disturbances in a uniform bubbly fluid. Int. J. Multiphase Flow 16, 211–231.

Brenner, M.P., 1999. Screening mechanisms in sedimentation. Phys. Fluids 11, 754–772.

Brown, S.N., Stewartson, K., 1978. On finite amplitude Benard convection in a cylindrical container. Proc. Roy. Soc. Lond. A 360, 455–469.

Busse, F.H., 1978. Non-linear properties of thermal convection. Rep. Prog. Phys. 41, 1929–1967.

Busse, F.H., 1985. Transition to turbulence in Rayleigh–Benard convection. In: Swinney, H.L., Gollub, J.P. (Eds.), Hydrodynamic Instabilities and the Transition to Turbulence. Springer, New York, pp. 97–137.

Catton, I., Edwards, D.K., 1967. Effect of side walls on natural convection between horizontal plates heated from below. J. Heat Transf. 89, 295–299.

Chandrasekhar, S., 1961. Hydrodynamic and Hydromagnetic Stability. Oxford University Press.

Charlson, G.S., Sani, R.L., 1970. Thermoconvective instability in a bounded cylindrical fluid layer. Int. J. Heat Mass Transf. 13, 1479–1496.

Chen, J.J.J., Jamialahmadi, M., Li, S.M., 1989. Effect of liquid depth on circulation in bubble columns: a visual study. Chem. Eng. Res. Des. 67, 203–207.

Chen, M.H., Cardoso, S.S.S., 2000. The mixing of liquids by a plume of low Reynolds number bubbles. Chem. Eng. Sci. 55, 2585–2594.

Chen, R.C., Reese, J., Fan, L.S., 1994. Flow structure in a three-dimensional bubble column and three-phase fluidized bed. AIChE J. 40, 1093–1104.

Climent, E., 2001. Institute of Fluid Mechanics, Louis Pasteur University of Strasbourg, Strasbourg, France, personal communication.

Climent, E., Magnaudet, J., 1999. Large-scale simulations of bubble-induced convection in a liquid layer. Phys. Rev. Lett. 82, 4827–4830.

Davis, R.H., 1996. Hydrodynamic diffusion of suspended particles: a symposium. J. Fluid Mech. 310, 325–335.

Davis, R.H., Birdsell, K.H., 1996. Hindered settling of semidilute monodisperse and polydisperse suspensions. AIChE J. 34, 123–129.

Davis, S.H., 1967. Convection in a box: linear theory. J. Fluid Mech. 30, 465–478.

Deckwer, W.D., 1992. Bubble Column Reactors. J. Wiley, Chichester.

Didwania, A.K., Homsy, G.M., 1981. Rayleigh–Taylor instabilities in fluidized beds. Ind. Eng. Chem. Fund. 20, 318–323.

Drazin, P.G., Reid, W.H., 1981. Hydrodynamic Stability. Cambridge University Press.

Eames, I., Belcher, S.E., Hunt, J.C.R., 1994. Drift, partial drift and Darwin's proposition. J. Fluid Mech. 275, 201–223.

UNCORRECTED PROOF

732 Edwards, D.K., 1969. Suppression of cellular convection by lateral walls. J. Heat Transf. 91, 145–150.
733 Franz, K., Borner, T., Kantorek, H.J., Buchholz, R., 1984. Flow structures in bubbly columns. Ger. Chem. Eng. 7,
734 365–374.
735 Hartline, B.K., Lister, C.R.B., 1977. Thermal convection in a Hele–Shaw cell. J. Fluid Mech. 79, 379–389.
736 Hills, J.H., 1974. Radial non-uniformity of velocity and voidage in a bubble column. Trans. Inst. Chem. Eng. 52, 1–9.
737 Jackson, R., 2000. The Dynamics of Fluidized Particles. Cambridge University Press.
738 Jeffreys, H., 1928. Some cases of instability in fluid motion. Proc. Roy. Soc. Lond. A 118, 195–208.
739 Joshi, J.B., Deshphande, N.S., Dinkar, M., Phanikumar, D.V., 2001. Hydrodynamic stability of multiphase reactors.
740 Adv. Chem. Eng. 26, 1–130.
741 Joshi, J.B., Sharma, M.M., 1979. A circulation cell model for bubble columns. Trans. Inst. Chem. Eng. 57, 246–251.
742 Joshi, J.B., Veera, U.P., Prasad, C.V., Phanikumar, D.V., Deshphande, N.S., Thakre, S.S., Thorat, B.N., 1998. Gas
743 hold-up structure in bubble column reactors. PINSA A 64, 441–567.
744 Kang, S.Y., Sangani, A.S., Tsao, H.K., Koch, D.L., 1997. Rheology of dense bubble suspensions. Phys. Fluids 9, 1540–
745 1561.
746 Kastanek, F., Zahradnik, J., Kratochvil, J., Cermak, J., 1993. Chemical Reactors for Gas–Liquid Systems. Ellis
747 Horwood, Chichester.
748 Kimura, R., Iga, K., 1995. Bubble convection. In: Redondo, J.M., Metais, O. (Eds.), Mixing in Geophysical Flows.
749 CIMNE, Barcelona, pp. 35–51.
750 Koschmieder, E.L., 1993. Benard Cells and Taylor Vortices. Cambridge University Press.
751 Kynch, G.J., 1952. A theory of sedimentation. Trans. Farad. Soc. 48, 166–176.
752 Lammers, J.H., Biesheuvel, A., 1996. Concentration waves and the instability of bubbly flows. J. Fluid Mech. 328, 67–
753 93.
754 Landau, L., Lifshitz, E.M., 1997. Fluid Mechanics. Butterworth–Heinemann, Oxford.
755 Lapin, A., Lubbert, A., 1994. Numerical simulation of the dynamics of two-phase gas–liquid flows in bubble columns.
756 Chem. Eng. Sci. 49, 3661–3674.
757 Medlin, J., Wong, H.W., Jackson, R., 1974. Fluid mechanical description of fluidized beds. Convective instabilities in
758 bounded beds. Ind. Eng. Chem. Fund. 13, 247–259.
759 Minev, P.D., Lange, U., Nandakumar, K., 1999. A comparative study of two-phase flow models relevant to bubble
760 column dynamics. J. Fluid Mech. 394, 73–96.
761 Mudde, R.F., van den Akker, H.E.A., 1999. Dynamic behaviour of the flow field of a bubble column at low to
762 moderate gas fractions. Chem. Eng. Sci. 54, 4921–4927.
763 Pellew, A., Southwell, R.V., 1940. On maintained convective motions in a fluid heated from below. Proc. Roy. Soc.
764 Lond. A 176, 312–343.
765 Prince, M.J., Blanche, H.W., 1990. Bubble coalescence and break-up in air-sparged bubble columns. AIChE J. 36,
766 1485–1499.
767 Rayleigh, L., 1916. On convection currents in a horizontal layer of fluid, when the higher temperature is on the under
768 side. Philos. Mag. 32, 529–546.
769 Richardson, J.F., Zaki, W.N., 1954. Sedimentation and fluidization: Part I. Trans. Inst. Chem. Eng. 32, 35–53.
770 Rothman, D.H., Kadanoff, L.P., 1994. Bubble, bubble, boil and trouble. Comput. Phys. 8, 199–204.
771 Ruzicka, M.C., 2000. On bubbles rising in line. Int. J. Multiphase Flow 26, 1141–1181.
772 Ruzicka, M.C., Zahradnik, J., Drahoš, J., Thomas, N.H., 2001a. Homogeneous–heterogeneous regime transition in
773 bubble columns. Chem. Eng. Sci. 56, 4609–4626.
774 Ruzicka, M.C., Drahoš, J., Fialova, M., Thomas, N.H., 2001b. Effect of bubble column dimensions on flow regime
775 transition. Chem. Eng. Sci. 56, 6117–6124.
776 Segel, L.A., 1969. Distant side-walls cause slow amplitude modulation of cellular convection. J. Fluid Mech. 38, 203–
777 224.
778 Shnip, A.I., Kolhatkar, R.V., Swamy, D., Joshi, J.B., 1992. Criteria for the transition from the homogeneous to the
779 heterogeneous regime in two-dimensional bubble column reactors. Int. J. Multiphase Flow 18, 705–726.
780 Stork, K., Muller, U., 1972. Convection in boxes: experiments. J. Fluid Mech. 54, 599–611.
781 Stork, K., Muller, U., 1975. Convection in boxes: an experimental investigation in vertical cylinders and annuli. J. Fluid
782 Mech. 71, 231–240.

UNCORRECTED PROOF

783 Tong, P., Ackerson, B.J., 1998. Analogies between colloidal sedimentation and turbulent convection at high Prandtl
784 numbers. Phys. Rev. E 58, R6931–R6934.
785 Tory, E.M., 2000. Stochastic sedimentation and hydrodynamic diffusion. Chem. Eng. J. 80, 81–89.
786 Tritton, D., 1988. Physical Fluid Dynamics. Clarendon Press, Oxford.
787 Turner, J.S., 1979. Buoyancy Effects in Fluids. Cambridge University Press.
788 Wallis, G.B., 1969. One-Dimensional Two-Phase Flow. McGraw-Hill, New York.
789 Whitham, G.B., 1974. Linear and Nonlinear Waves. J. Wiley, New York.
790 van Wijngaarden, L., Kapteyn, C., 1990. Concentration waves in dilute bubble/liquid mixtures. J. Fluid Mech. 212,
791 111–137.
792 Yuan, H., Prosperetti, A., 1994. On the in-line motion of two spherical bubbles in a viscous fluid. J. Fluid Mech. 278,
793 325–349.
794 Zahradnik, J., Fialova, M., Ruzicka, M., Drahoš, J., Kastanek, F., Thomas, N.H., 1997. Duality of the gas–liquid flow
795 regimes in bubble column reactors. Chem. Eng. Sci. 52, 3811–3826.

UNCORRECTED PROOF